Supporting Information

DNA-guided confined growth of bimetallic nanoclusters for constructing a multienzyme-integrated nanoplatform

Min Yang [a], Longjiao Zhu[a] *, Yushi Xie[a], Xiangyang Li[b], Xuan Ma[a], Yifan Wu[a], Zaihui Du[a], Qian Yang[c], Wentao Xu [a] *

a Food Laboratory of Zhongyuan, Key Laboratory of Precision Nutrition and Food Quality, Beijing Laboratory for Food Quality and Safety, Key Laboratory of Safety Assessment of Genetically, Modified Organism (Food Safety), Department of Nutrition and Health, China Agricultural University, Beijing 100193, China

b Beijing Laboratory of Food Quality and Safety, Beijing Key Laboratory of Agricultural Product Detection and Control of Spoilage Organisms and Pesticide Residue, Key Laboratory of Agricultural Product Processing and Quality Control (Co-construction by Ministry and Province), Faculty of Food Science and Engineering, Beijing University of Agriculture, Beijing, 102206, China

c School of Public Health, Hebei Key Laboratory of Public Health Safety, Hebei University, Baoding, 071002, China

** Corresponding author：*

Wentao Xu; E-mail: xuwentao@cau.edu.cn.
Longjiao Zhu; E-mail: zhulongjiao@126.com.

Materials and method

Chemicals and materials

Gold (III) chloride trihydrate ($HAuCl_4 \cdot 3H_2O$), sodium borohydride ($NaBH_4$), chloroplatinic acid hexahydrate ($H_2PtCl_6 \cdot 6H_2O$, 99.9%), and 30% H_2O_2 were purchased from Sigma-Aldrich (Beijing, China). 3,3′,5,5′-tetramethylbenzidine (TMB), *o*-phenylenediamine (OPD), 2,2'-azino-bis (3-ethylbenzothiazoline-6-sulfonic acid) (ABTS) were purchased from Macklin Biochemical Co., Ltd. (China). Streptavidin Magnetic Beads (SA-MB) was purchased from MedChemExpress (Shanghai, China). All solutions were prepared with Millipore water. All oligonucleotides in this study were synthesized by Shanghai Sangon Biotechnology Co., Ltd. (Shanghai, China) and were purified by HPLC. The sequences are shown in Table S1 (Supporting Information).

Instruments

An ultraviolet-visible light (UV-vis) spectrophotometer was used to measure UV-vis absorption spectra (TU-1901, Beijing Persee General Instrument, China). Absorption spectra were recorded on a microplate reader (SYNERGYHTX, BioTek, USA). high-resolution transmission electron microscope (HRTEM) was used to characterize analysis DNA-Au/Pt nanozyme (Talos F200X, FEI, America). The hydrodynamic particle size and zeta-potential were measured using a nanoparticle size and zeta potentiometer (Zetasizer Nano ZS90, Malvern Instruments, UK). The chemical composition and state of elements present in the Fe-DNA nanozymes were characterized via XPS (ESCALAB 250Xi, Thermo Fisher, USA). X-ray diffraction (XRD) analysis was performed on a Rigaku Dmax-2000 diffractometer (Bruker Co., Germany). Room-temperature Fourier transform infrared (FT-IR) spectra were recorded using a Spectrum 100 FT-IR spectrometer in the region of 4000-500 cm^{-1} (Spectrum 100, PerkinEImer, China). The concentration of nucleic acids is analyzed using NanoDrop One microUV-visible spectrophotometer (Thermo Fisher, USA).

Experimental section

Synthesis of DNA-Au/Pt Nanozymes

Chemical reduction method: Mix 8 μL of $HAuCl_4 \cdot 3H_2O$ and $H_2PtCl_6 \cdot 6H_2O$ (both at 1mM) with 5 μL of DNA template (100 μM, 5'-CCCCCCCCCCCC-3') in 71 μL of phosphate buffer (10mM, pH 6.6). Incubate at 30°C for 15 minutes, then add 8 μL of $NaBH_4$ (3mM). Shake vigorously for 1 minute and incubate in the dark for 6h. All DNA-Au/Pt nanoclusters were purified using Amicon® Ultra 3K centrifugal filters and subsequently resuspended in an equal volume (e.g., 100 μL) of 10 mM phosphate buffer (pH 6.6). The final concentration was determined based on the concentration of the encapsulated DNA.

High-temperature heating method: Mix 8 μL of $HAuCl_4 \cdot 3H_2O$ and $H_2PtCl_6 \cdot 6H_2O$ (both at 1mM) with 5 μL of DNA template (100 μM, 5'-CCCCCCCCCCCC-3') in 79 μL of phosphate buffer (20mM, pH 6.6). The mixture was then heated at 95 °C for 5 minutes, using the high temperature to promote the reduction of metal ions and the formation of nanoparticles.

Ultraviolet irradiation Method: Mix 8 μL of $HAuCl_4 \cdot 3H_2O$ and $H_2PtCl_6 \cdot 6H_2O$ (both at 1mM) with 5 μL of DNA template (100 μM, 5'-CCCCCCCCCCCC-3') in 79 μL of phosphate buffer (20mM, pH 6.6). Expose to ultraviolet radiation for 5 minutes.

For all the above products, centrifuge at 12,000 rpm and store at room temperature for after use.

Peroxidase-like (POD-like) activity assay of DNA-Au/Pt Nanozymes

The peroxidase-like activity of the DNA-Au/Pt nanozymes (5μM) was evaluated through the catalytic oxidation of TMB in the presence of H_2O_2 in an HAc-NaAc solution. Typically, 5 μL DNA-Au/Pt nanozymes (phosphate buffer, 10mM, pH 6.6) was added into reaction system (130 μL 25 mM HAc-NaAc, pH 4.0) containing 40 μL 4 mM TMB and 20 μL 500 mM H_2O_2, followed by 5 min incubation at room temperature. Finally, the mixture was transferred into a 96-well plate and the color change was studied spectrographically by recording the absorbance spectrum at 500 nm-750nm. The peroxidase-like activity of the Fe-DNA nanozymes was also investigated with another peroxidase substrate OPD and ABTS under the same conditions.

Steady-State Kinetics Assay

The steady-state kinetic assays of the POD-like activity of 5 μL, 5μM DNA-Au/Pt nanozymes (phosphate buffer, 10mM, pH 6.6) were performed via varying TMB concentrations (0.2-20 mM) at both a constant H_2O_2 concentration (20 mM) and changing H_2O_2 concentrations (0.02-1 mM) at a constant TMB concentration (1.0 mM). The apparent kinetic parameters (K_m and V_{max}) were calculated according to the Michaelis-Menten saturation curve.

Detection of superoxide anion radicals $O_2^{\bullet-}$

To verify whether $O_2^{\bullet-}$ was generated in the catalytic process, dihydroethidium (DHE) was selected as the capture probe for $O_2^{\bullet-}$. Typically, 10 μL nanozymes was added into 960 μL HAc-NaAc buffer containing 5 μL 2 mM DHE and 20 μL 500 mM H_2O_2, and the fluorescence spectrum were subsequently recorded. P-benzoquinone (p-BQ) was used as a scavenger to detect $O_2^{\bullet-}$ by measuring the catalytic activity of the DNA-Au/Pt nanozymes.

Detection of hydroxyl radicals ·OH

To verify whether ·OH was generated in the catalytic process, Terephthalic acid (TA) was selected as the capture probe for ·OH. Typically, 10 μL DNA-Au/Pt nanozymes was added into 200 μL HAc-NaAc buffer (25 mM, pH 4.0) containing 5mM TA and 20 μL 500 mM H_2O_2, and the fluorescence spectrum results were recorded. In addition, 2-propanol was used as a scavenger to detect ·OH by measuring the catalytic activity of the DNA-Au/Pt nanozymes.

Stability of DNA-Au/Pt Nanozymes

In the pH stability experiments, we treated the DNA-Au/Pt nanozymes (5 μL, 5μM) with a series of HAc-NaAc solutions (130 μL 25 mM, pH 4.0) at varying pH (ranging from 3.0 to 9.0) for 60 min and then measured their POD-like activity. For thermal stability testing, the 5 μL, 5μM DNA-Au/Pt nanozymes (phosphate buffer, 10mM, pH 6.6) were subjected to a range of different temperature conditions (from -20℃ to 110℃), after which their POD-like activity was investigated. To ensure storage stability, we recorded the POD-like activity of the DNA-Au/Pt nanozymes after storing them at room temperature for different periods (from 0 to 5 months). To comprehensively assess batch-to-batch stability, we synthesized 6 batches of DNA-Au/Pt nanozymes and evaluated their POD-like activity one by one as follows:

5 μL, 5μM DNA-Au/Pt nanozymes (phosphate buffer, 10mM, pH 6.6) was added into reaction system (130 μL 25 mM HAc-NaAc, pH 4.0) containing 40 μL 4 mM TMB and 20 μL 500 mM H_2O_2, followed by 5 min incubation at room temperature. Finally, the mixture was transferred into a 96-well plate and the color change was studied spectrographically by recording the absorbance at 625nm.

Preparation of MB-H

First, the H-substrate probe is denatured at 70°C for 3 min and then cooled at room temperature for at least 5 min. Take an appropriate amount of fully suspended SA-MBs (10 mg/mL) into a centrifugal tube for magnetic separation, and discard the supernatant. Add 200μL Buffer I (10 mM Tris-HCl, 1mM EDTA, 1M NaCl, 0.05% Tween 20, pH 7.5) washing magnetic beads, vortex oscillating for 15 seconds, magnetic separation to discard the supernatant, repeat washing magnetic beads once. Biotinated H substrate probe diluted with 200 μL Buffer I (final concentration 2μM) was added, fully oscillated and suspended, and incubated at room temperature on a rotating mixer for 30 min. Magnetic separation, discard the supernatant, add 200 μL Buffer I, repeat washing magnetic beads twice, remove the unbound sequence. The precipitation was collected, the bead-allosteric probe complex was re-suspended with 100 μL Binding buffer, and stored in a refrigerator at 4 ℃ for later use.

Native polyacrylamide gel electrophoresis (PAGE)

A 12% PAGE was prepared to verify the cleavage of DNAzyme. The samples including 500nM Target, 500nM DNAzyme, and 500nM H DNA were incubated in 4 × TE buffer (40 mM Tris-HCl, 4 mM EDTA, pH = 7.5) with 150 mM Mg^{2+} at 28°C for 2 h. 10 μL of samples mixed with loading buffer was then loaded into the polyacrylamide gel. Electrophoresis was implemented at 135 V for 1 h. The gel slabs were subsequently stained with the GelRed solution in the dark for 10 min. Finally, the fluorescence images were recorded using a FluorChem FC3 imaging system (FluorChem FC3, Protein Simple, California, USA)

Colorimetric analysis of miR-21

First, the DNAzyme were denatured at 95 °C for 3 min and cooled down in their corresponding buffer mentioned above under a ramp annealing protocol (from 95°C to 4°C over a period of 35 min. Subsequently, the MB-H was added to the DNAzyme solutions. Different concentrations of miR-21 were then added to the above solutions, with the final concentrations: 0.01,0.05,0.1,0.5,1,5,10,50,100 nM. The final volume was 100 μL(containing 100nM DNAzyme,1μM MB-H) and the reaction mixture was kept in 90 min at 28 °C. The sample was shaken and mixed every 10 minutes during incubation. Then it was magnetically separated, washed three times with Buffer I, and re-suspended in 100 μL PB buffer, taking 5μL as a template to synthesize DNA-Au/Pt. Finally, the peroxidase activity of the aforementioned solution was assessed.

Catalase and laccase activities assay

The catalase activity was measured by a Catalase Assay Kit (Beyotime, China). The laccase-like activity of the nanozymes was evaluated using 2,4-dichlorophenol (2,4-DP) as the substrate and 4-aminoantipyrine (4-AP) as the chromogenic agent. The assay measures the colorimetric reaction between phenolic compounds and 4-AP. Briefly, a mixture containing 100 μL of 2,4-DP (1 mg/mL), 100 μL of 4-AP (1 mg/mL), and 200 μL of water was prepared. Then, 20 μL of DNA-Au/Pt nanozymes was added to the mixture. The reaction was allowed to proceed at room temperature for 5 minutes. Finally, the ultraviolet absorption spectrum at a wavelength of 510 nm was recorded.

Catalytic Degradation of malachite green

The MG dye was dissolved in water, and a reaction mixture was prepared by adding 45 μL of 0.1 mg/mL MG, 20 μL of H_2O_2 (500 mM), and 15 μL of DNA-Au/Pt to 190 μL of water. After a specified reaction time, the characteristic absorbance peak of MG at 618 nm was analyzed using a microplate reader.

Statistical Analysis

All experiments were conducted with a minimum of three biological replicates. Statistical analyses were carried out using GraphPad Prism 7. P values were calculated using unpaired Student's t-test for two groups or one-way ANOVA for more than two groups. A p value less than 0.05 was considered statistically significant. Data are presented as Mean ± SD (standard deviation). *$p < 0.1$, **$p < 0.01$, ***$p < 0.001$, ****$p < 0.0001$, ns (no significance).

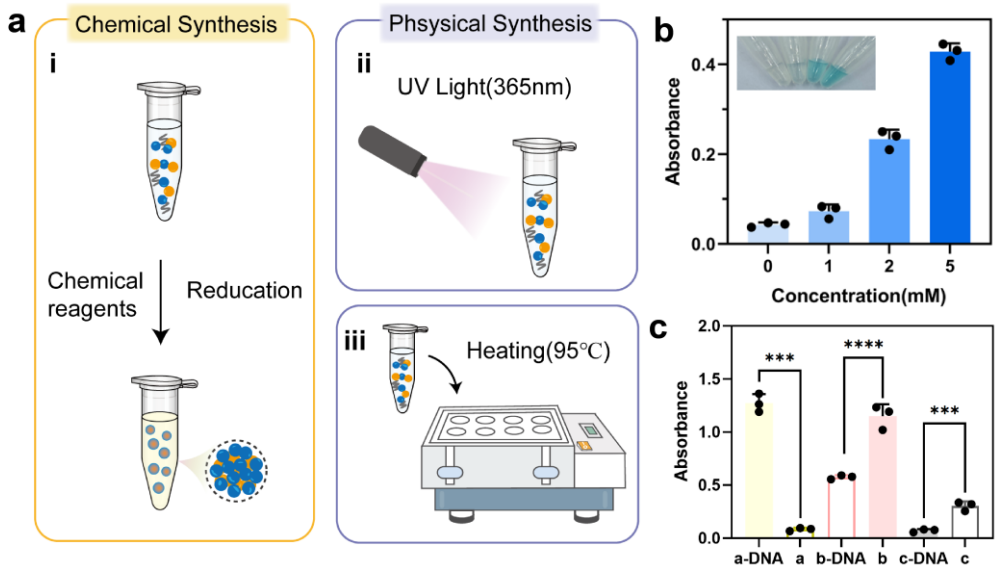

Fig. S1 Oxidation of TMB by different concentrations of gold and platinum ions. (a) Schematic diagram of three synthesis methods (i: chemical reduction method; ii: UV irradiation method; iii: high-temperature heating method). (b) Oxidation of TMB by different concentrations of gold and platinum ions (measured at 652 nm). (c) Comparison of POD-like activity among three synthesis methods (a: chemical reduction method; b: UV irradiation method; c: high-temperature heating method), with and without DNA (measured at 652 nm using TMB as the substrate). All data are presented as mean ± SD. Statistical significance was calculated by two-tailed unpaired *t* test in (c) *** $p < 0.01$; **** $p < 0.0001$

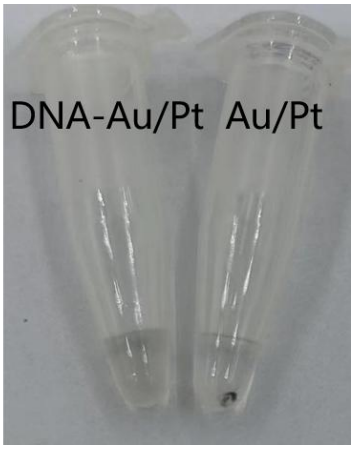

Fig. S2 Photograph of DNA-Au/Pt and Au/Pt after centrifugation (DNA-Au/Pt NCs: no precipitate; Au/Pt NPs: black precipitate)

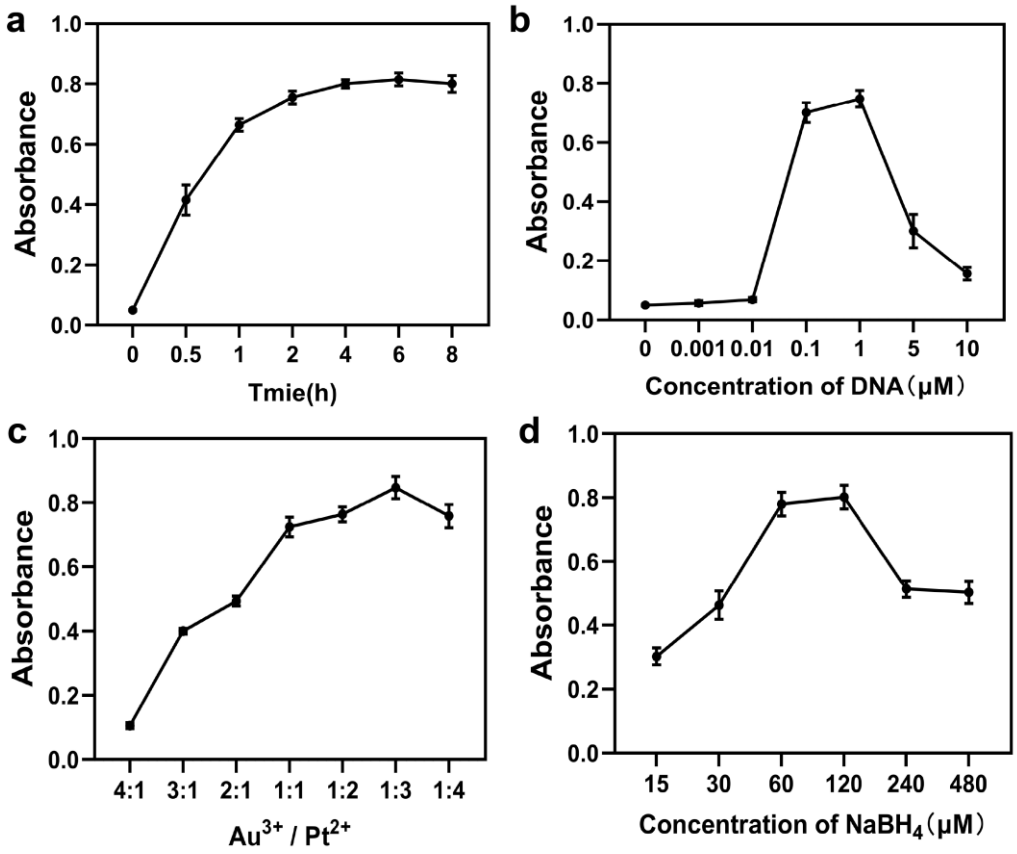

Fig.S3 The synthesis conditions of DNA-Au/Pt were optimized (measured at 652 nm using TMB as the substrate). (a) Time. (b) Concentration of DNA. (c) The proportion of metal ions. (d) The concentration of reducing agent $NaBH_4$

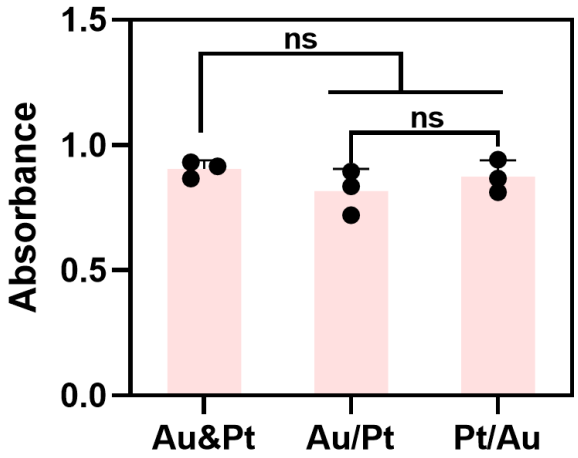

Fig.S4 Comparison of catalytic activity based on the addition sequence of metal ions measured at 652 nm using TMB as the substrate (Au&Pt: Co-addition; Au/Pt: Au-first addition; Pt/Au: Pt-first addition). All data are presented as mean ± SD. Statistical significance was calculated by one-way ANOVA with Tukey's multiple comparisons test. ns, not significant.

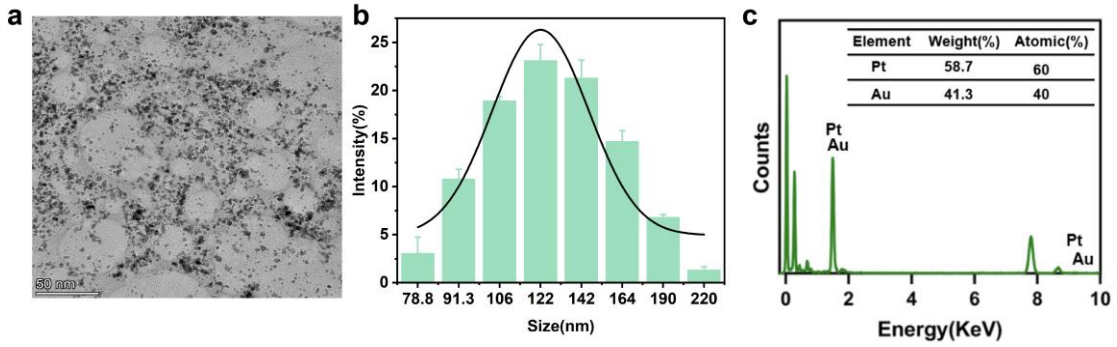

Fig. S5 Characterization of nanozymes. (a) HRTEM of DNA-Au/Pt. (b) Hydrodynamic diameter of Au/Pt NPs measured by dynamic light scattering (DLS). (c) EDS spectrum of DNA-Au/Pt (Inset: quantitative data of Pt and Au elements)

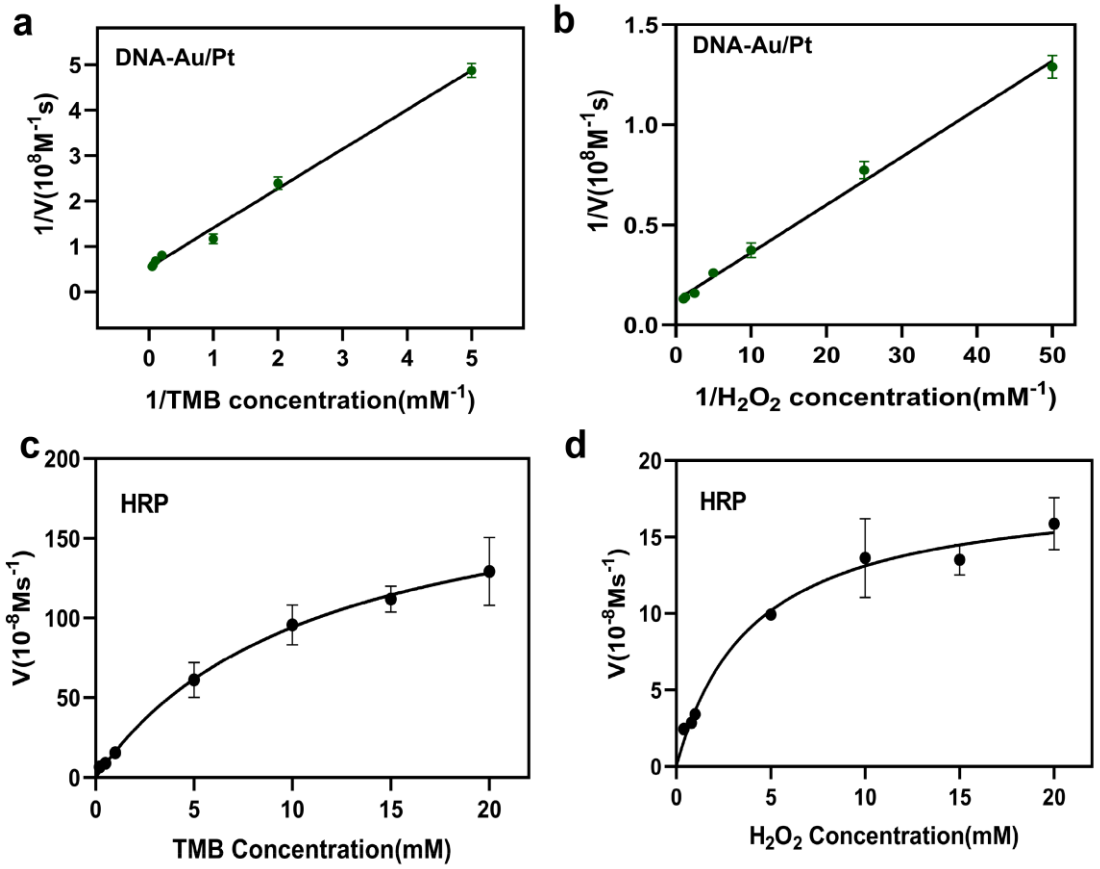

Fig. S6 Kinetic analysis of DNA-Au/Pt and HRP. (a)The Lineweaver-Burk plots of DNA-Au/Pt for TMB (Varying TMB concentration at a fixed H_2O_2 concentration). (b)The Lineweaver-Burk plots of DNA-Au/Pt for H_2O_2 (Varying H_2O_2 concentration at a fixed TMB concentration). Michaelis-Menten curves of HRP with TMB (c) and H_2O_2 (d) as substrates, respectively (HRP (5μL, 2 μg/mL), 25 mM HAc-NaAc solution (pH = 4.0), 10 min reaction). For panel c: H_2O_2 (20 mM); For panel d: TMB (1 mM)

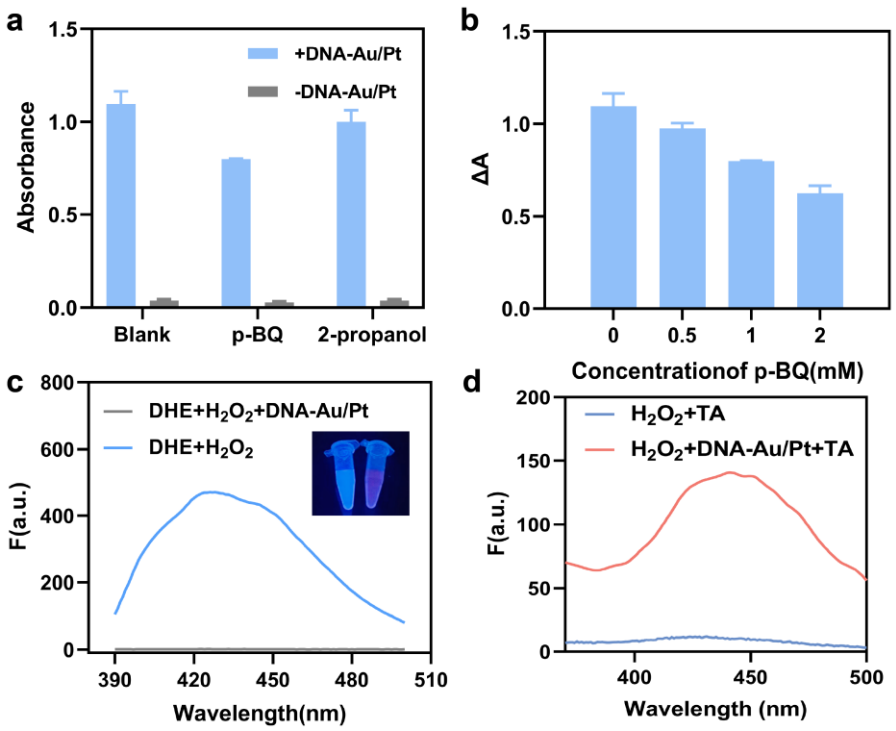

Fig. S7 Capture and scavenging of free radicals. (a) Inhibition of the catalytic reaction by various scavengers, as monitored by absorbance at 625 nm (using TMB as the substrate). (b) Concentration-dependent inhibition of DNA-Au/Pt catalyzed TMB oxidation by p-BQ (dissolve in DMSO). The absorbance was measured at 652 nm. Data were corrected for background using a solvent blank. (c) Detection of $O_2^{\bullet-}$ by DHE (Inset: left: DHE+H_2O_2; right: DHE+H_2O_2+DNA-Au/Pt). (d) Detection of •OH by TA

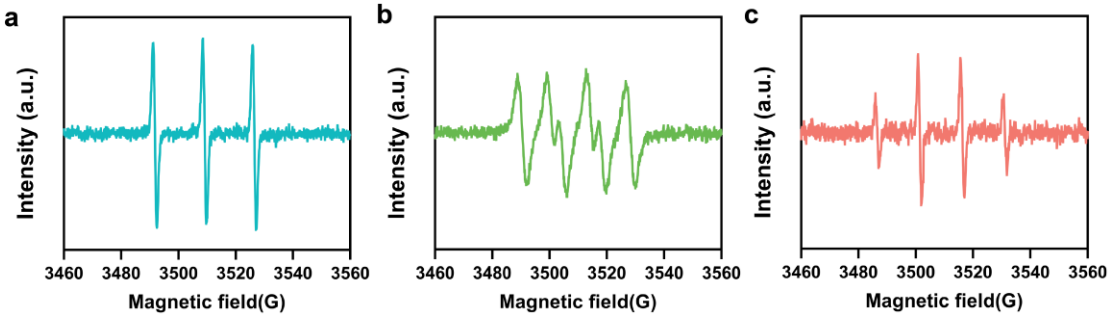

Fig. S8 EPR spectra of (a) $^1O_2$; (b) $O_2^{\bullet-}$; (c) •OH

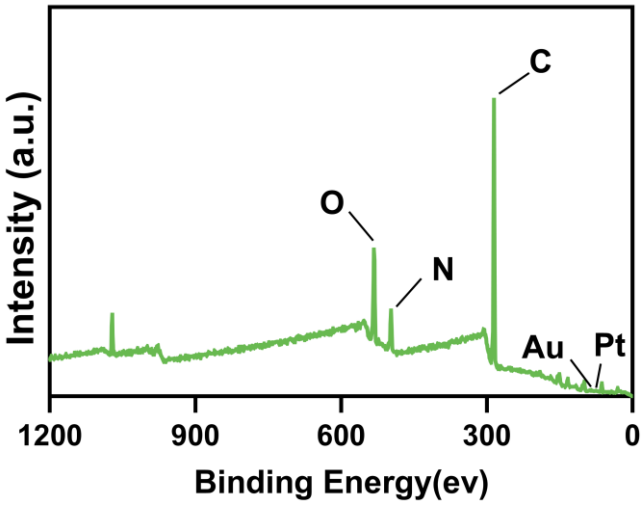

Fig. S9 XPS spectra of DNA-Au/Pt

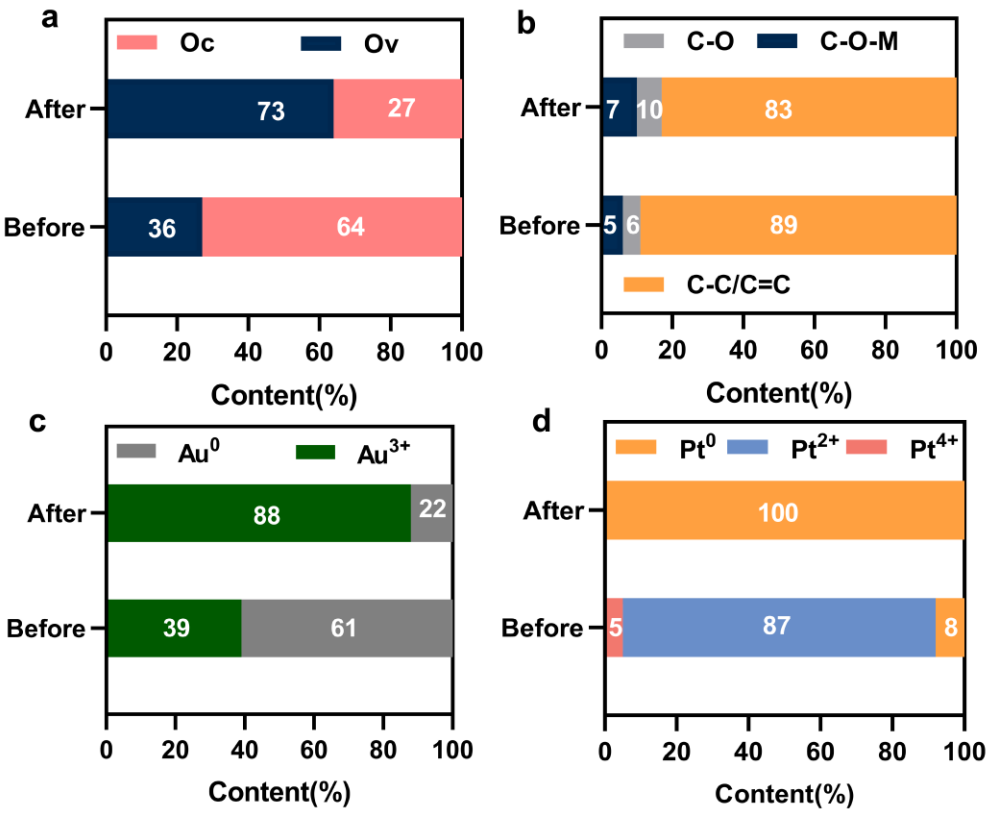

Fig. S10 The content of different types of (a)O;(b) C;(c) Au;(d) Pt in the DNA-Au/Pt before and after catalysis

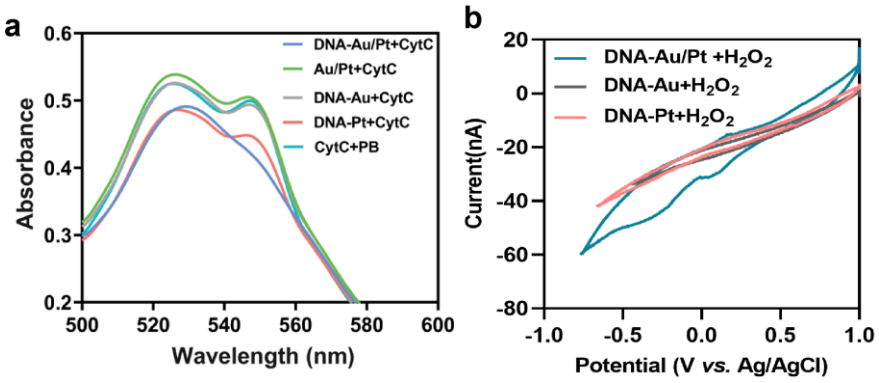

Fig. S11 Electron Transfer during DNA-Au/Pt Nanozyme Catalysis. (a) Ultraviolet visible absorption spectra of Cyt C and Cyt C reacted with different catalyst. (b) Cyclic voltammetry curves of DNA-Au, DNA- Pt and DNA-Au/Pt in the presence of 500mM H_2O_2

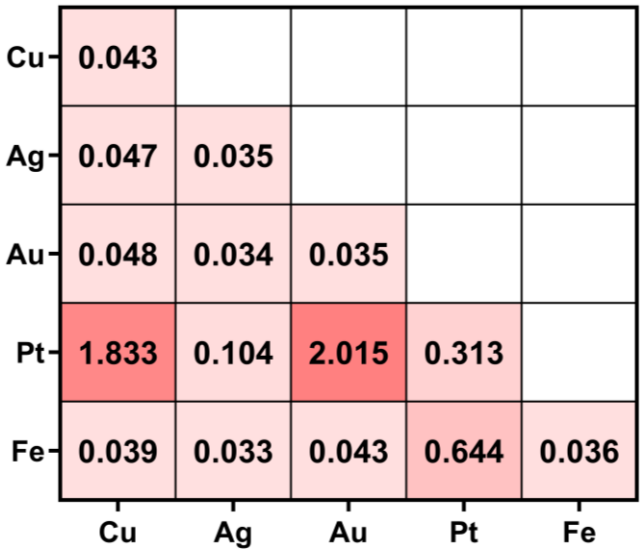

Fig. S12 Catalytic activity of bimetallic nanozymes formed by different metals (Absorbance: 625nm)

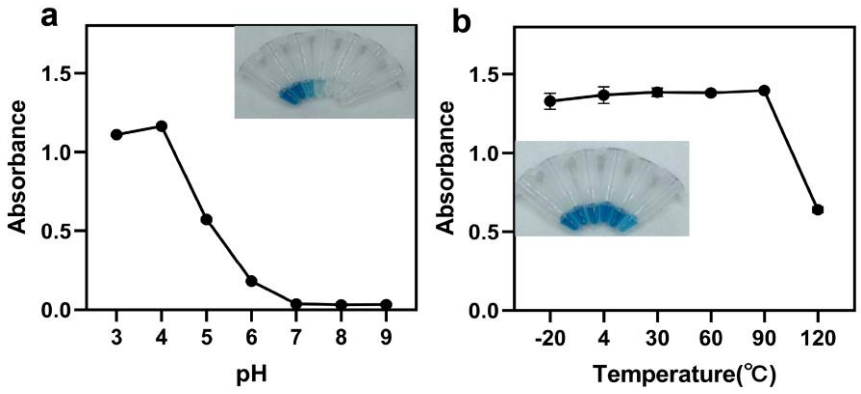

Fig. S13 Environmental tolerance of DNA-Au/Pt catalytic activity. (a) pH; (b) Temperature

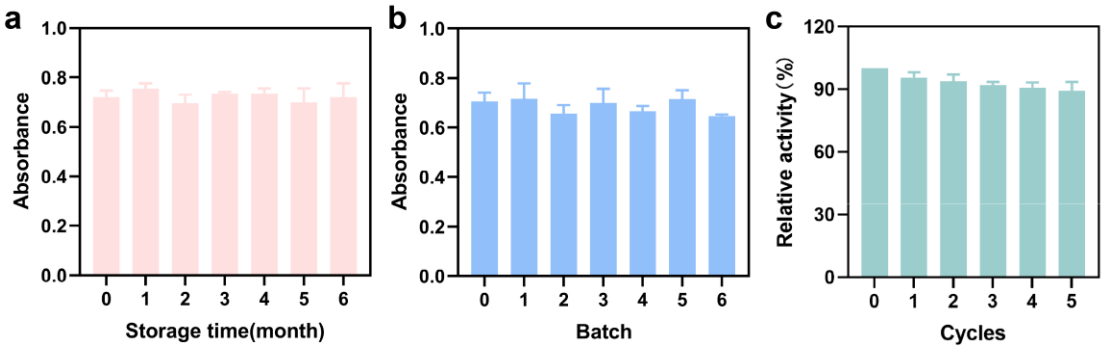

Fig. S14 Stability study of DNA-Au/Pt nanozyme. (a)The storage stability of Fe-DNA nanozyme in room temperature. (b)The batch stability of DNA-Au/Pt nanozyme. (c) The POD-like activity of DNA-Au/Pt after five catalytic cycles. Following each cycle, the nanozyme was recovered and purified using an Amicon® Ultra 3K centrifugal filter unit for the subsequent test. The error bars were obtained by three measurements. Data were presented as mean ± SD, n = 3

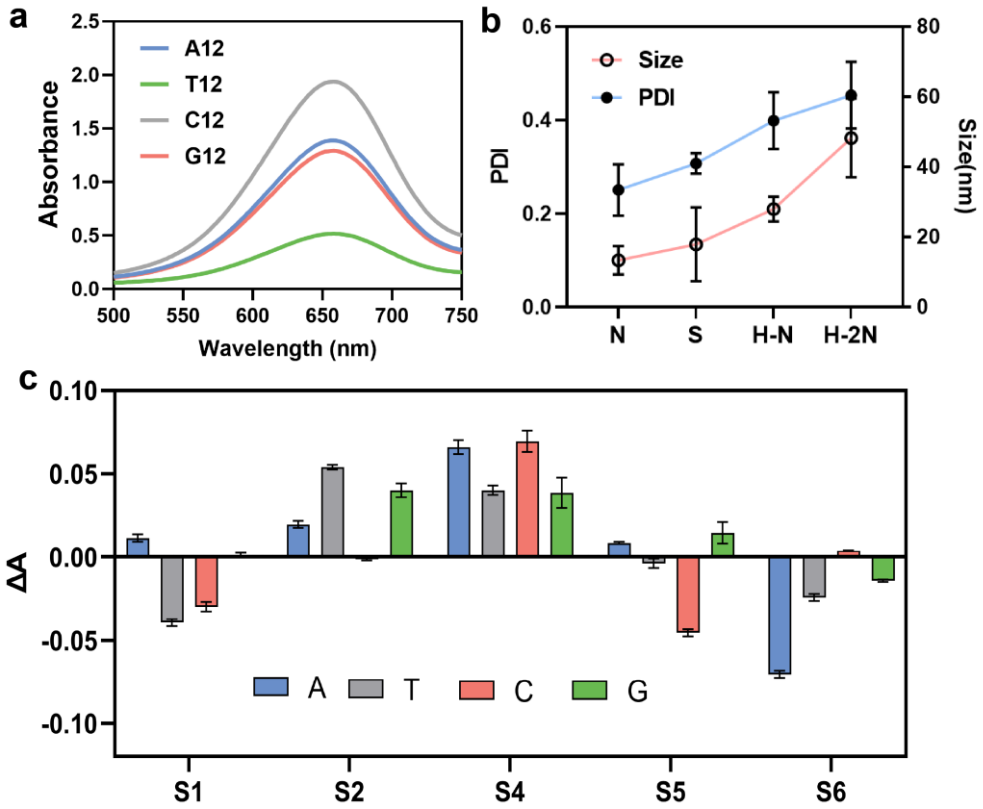

Fig. S15 Effect of DNA on catalytic properties of DNA-Au/Pt. (a) The effect of different base sequences (5μL, 100μM) as synthetic templates on DNA-Au/Pt enzyme activity. (b)The DLS analysis and PDI of DNA-Au/Pt nanozymes synthesized using H, S, H-N, and H-2N as nucleation sequences. (c)The influence of different bases on the enzyme activity of various nucleation sequences (measured at 652 nm using TMB as the substrate)

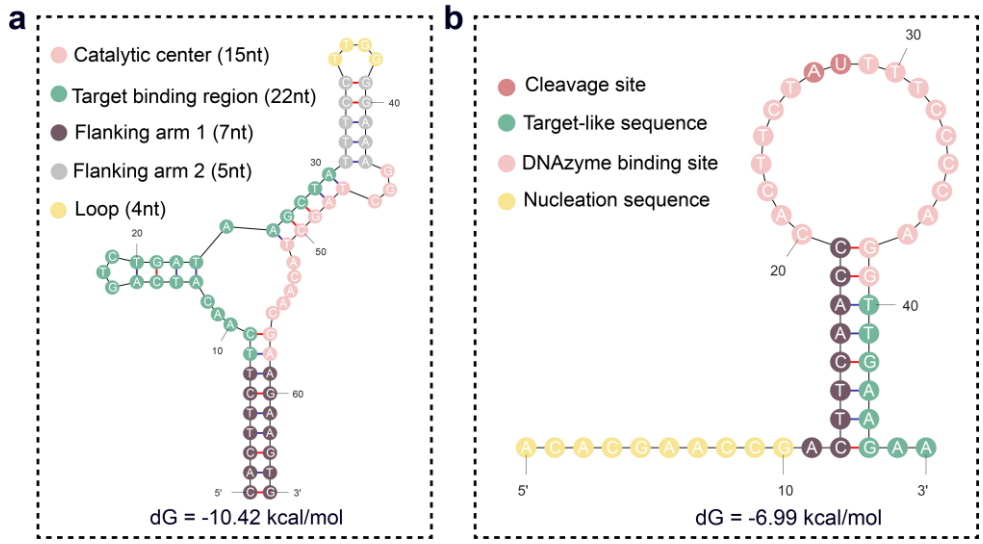

Fig. S16 Secondary structure. (a) Locked DNAzyme. (b) H DNA

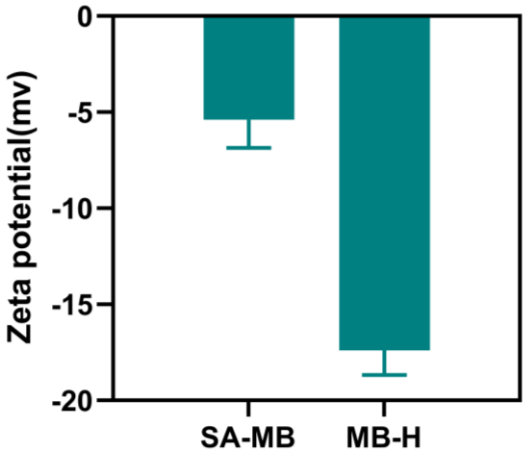

Fig.S17 Zeta potential before and after MB coupling with H DNA. Data were presented as mean ± SD, n = 100

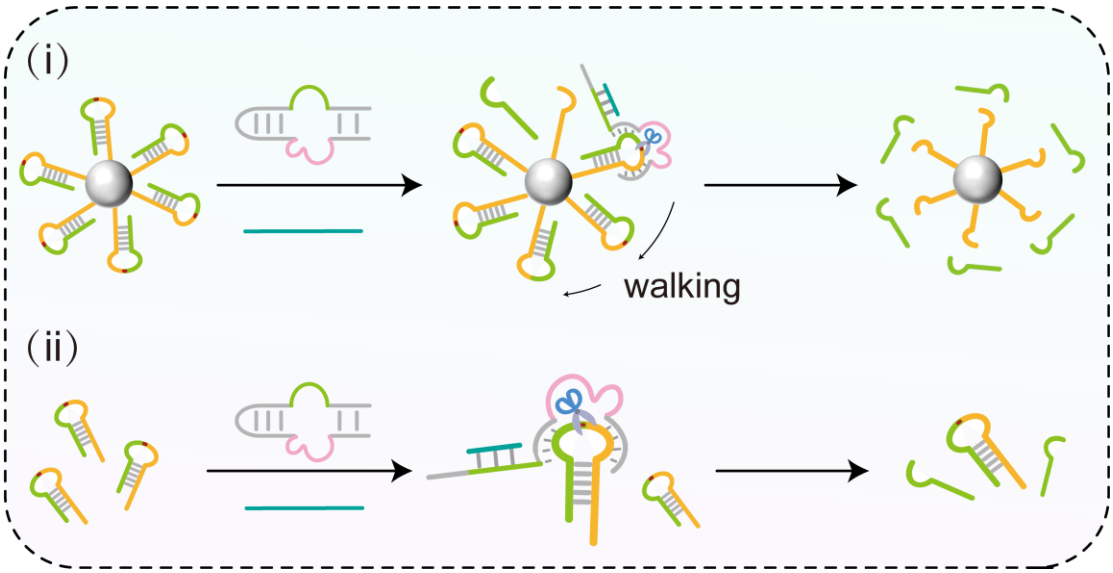

Fig.S18 Schematic diagram of walking and non-walking biosensor

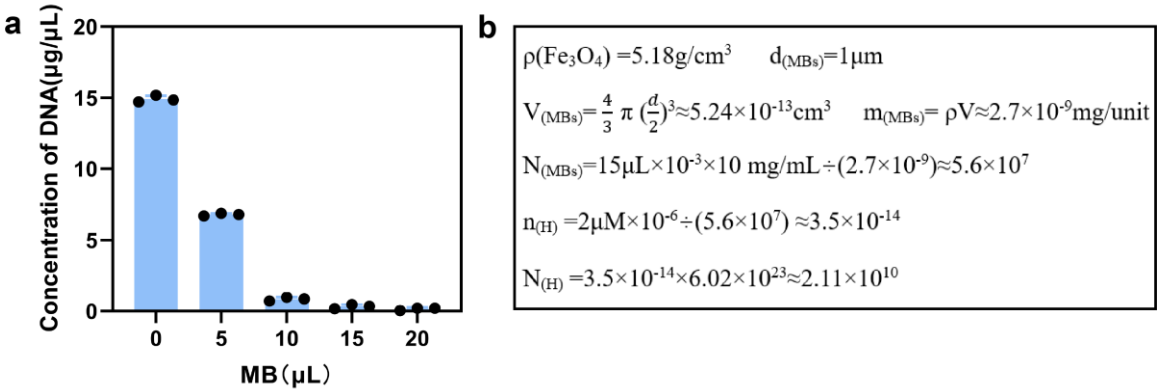

Fig. S19 (a)Optimization of the amount of MB. (b) The calculation process of the H1 number on magnetic bead. Data were presented as mean ± SD, n = 3

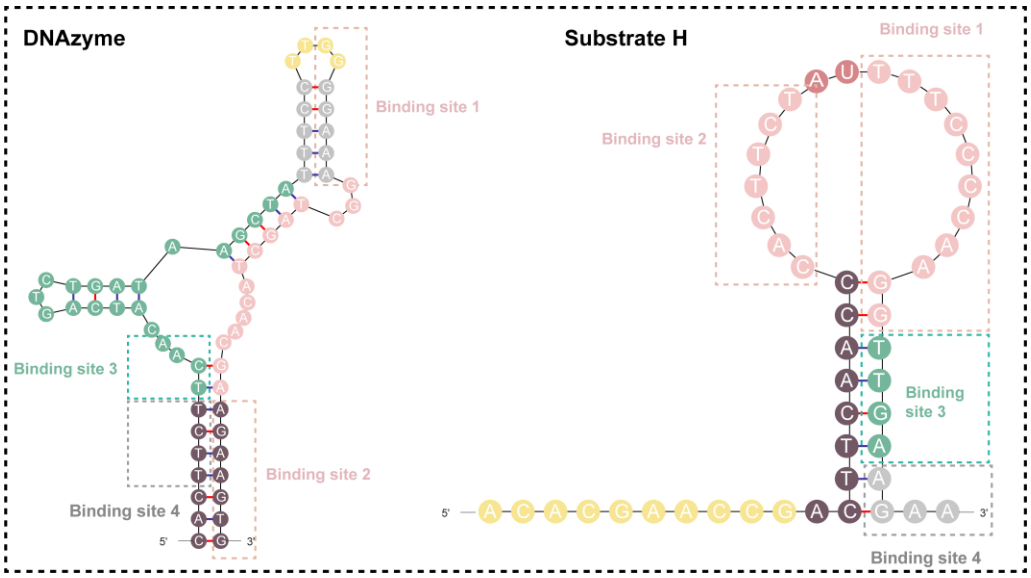

Fig. S20 Diagram of binding site of hairpin substrate H and DNAzyme.

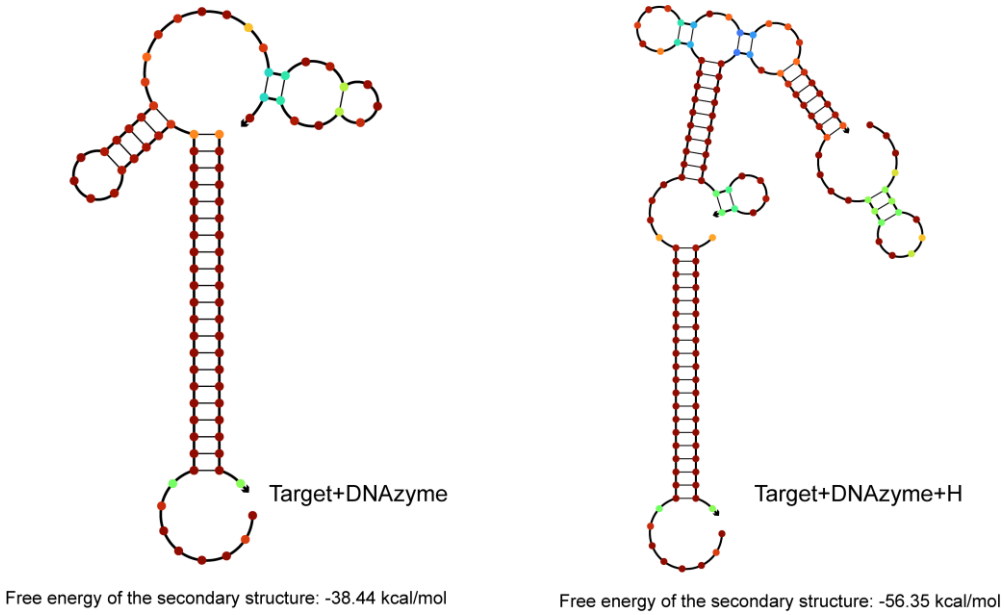

Fig. S21 Binding of target +DNAzyme (left) and target +DNAzyme +H (right), as suggested by NUPACK calculations

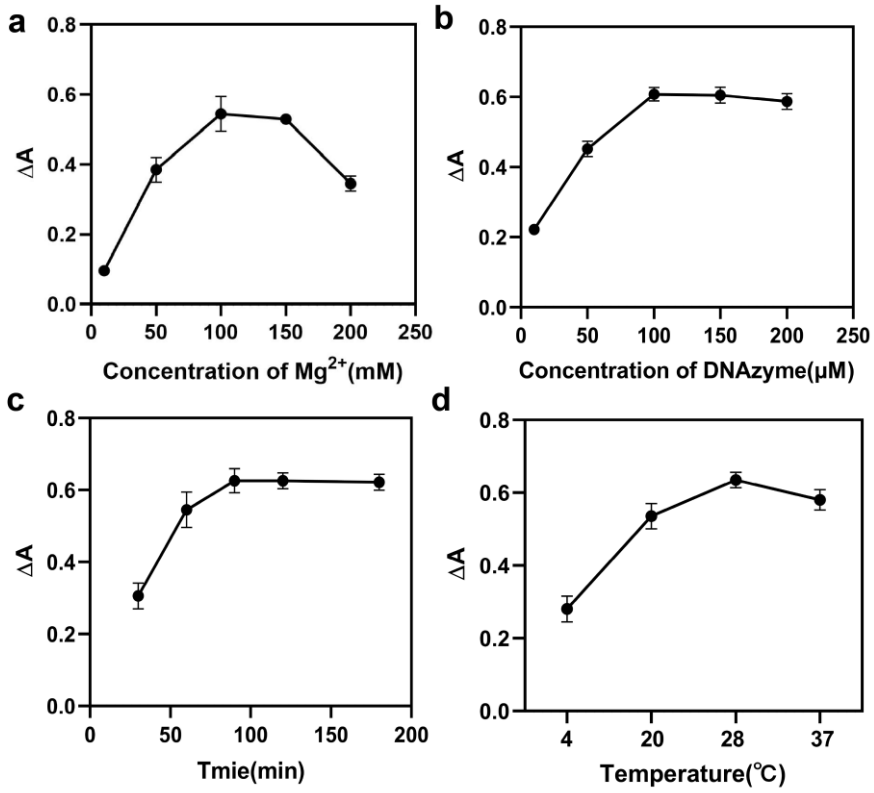

Fig. S22 Optimization of reaction conditions. (a) The concentration of Mg^{2+}. (b) The concentration of DNAzyme. (c) Reaction time. (d) Reaction temperature. Data were presented as mean ± SD, n = 3

Fig.S23 O_2 bubbles produced by different volumes of DNA-Au/Pt catalyzed H_2O_2(500mM, 1mL) solution for 5 min (from left to right: 0,10, 20, 40μL)

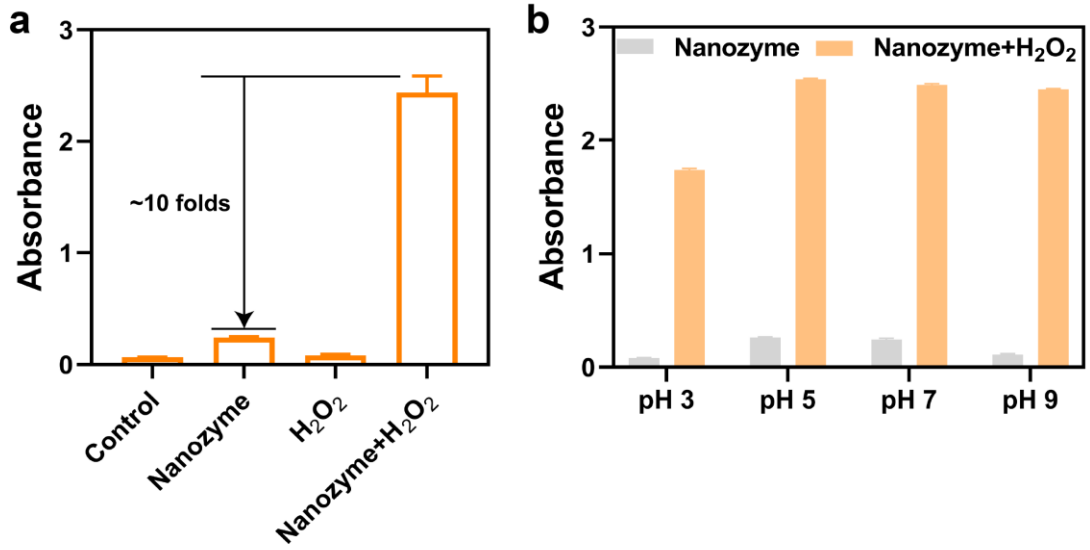

Fig. S24 Evaluation of laccase activity. (a) Comparison of laccase activity (Control: 2,4-DP+4-AP; Nanozyme+ 2,4-DP+4-AP; H_2O_2+2,4-DP+4-AP; Nanozyme+ H_2O_2+ 2,4-DP+4-AP). (b) Effect of pH on laccase activity

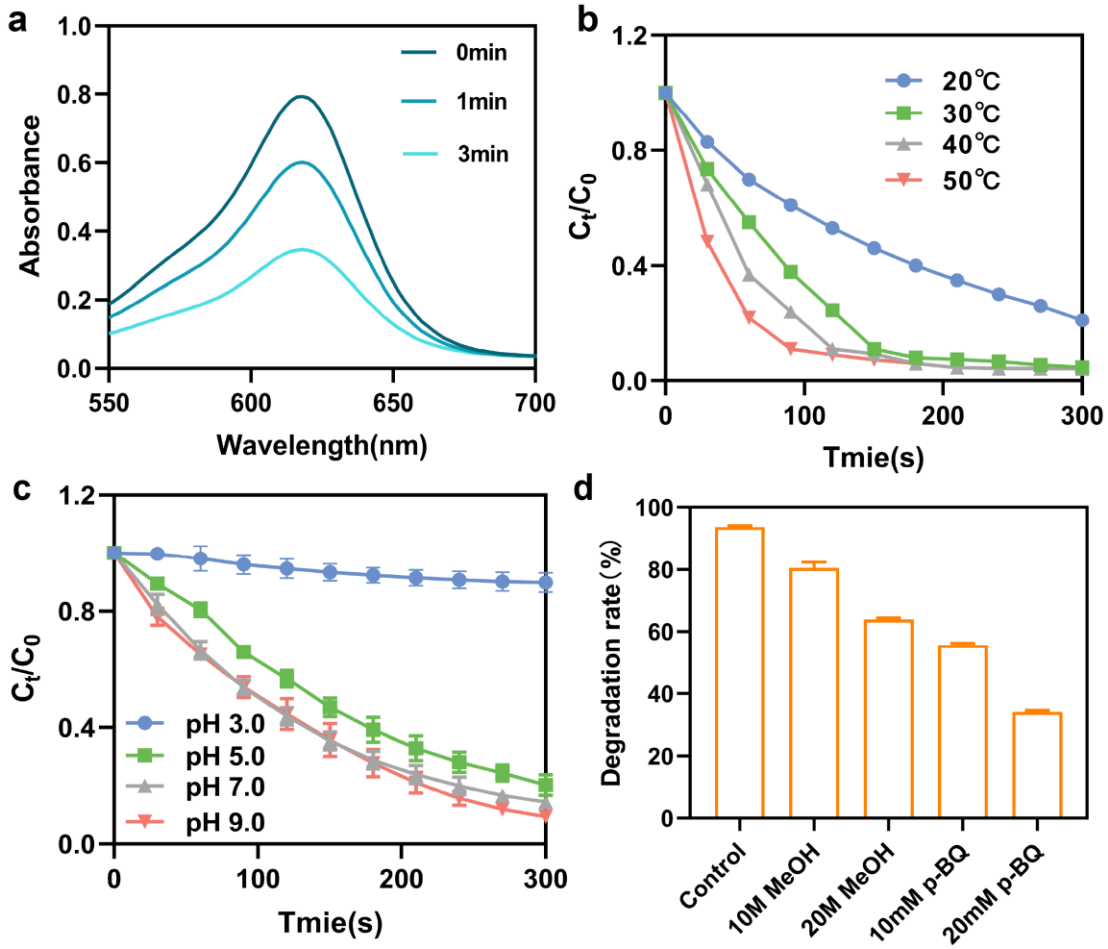

Fig. S25 Degradation performance of DNA-Au/Pt nanozyme on MG. Effects of reaction time(a), temperature(b), and pH Value (c) on MG Degradation by DNA-Au/Pt. (d) MG degradation performance by DNA-Au/Pt with or without ROS scavengers. (Control: nanozyme+H_2O_2+MG+H_2O;10mM MeOH: nanozyme+H_2O_2+MG+H_2O+ 10mM MeOH; 10mM MeOH: nanozyme+H_2O_2+MG+H_2O+20mMMeOH; 10mM p-BQ: nanozyme+H_2O_2+MG+H_2O+10mM p-BQ; 20mM p-BQ: nanozyme + H_2O_2+MG+H_2O+20mM p-BQ)

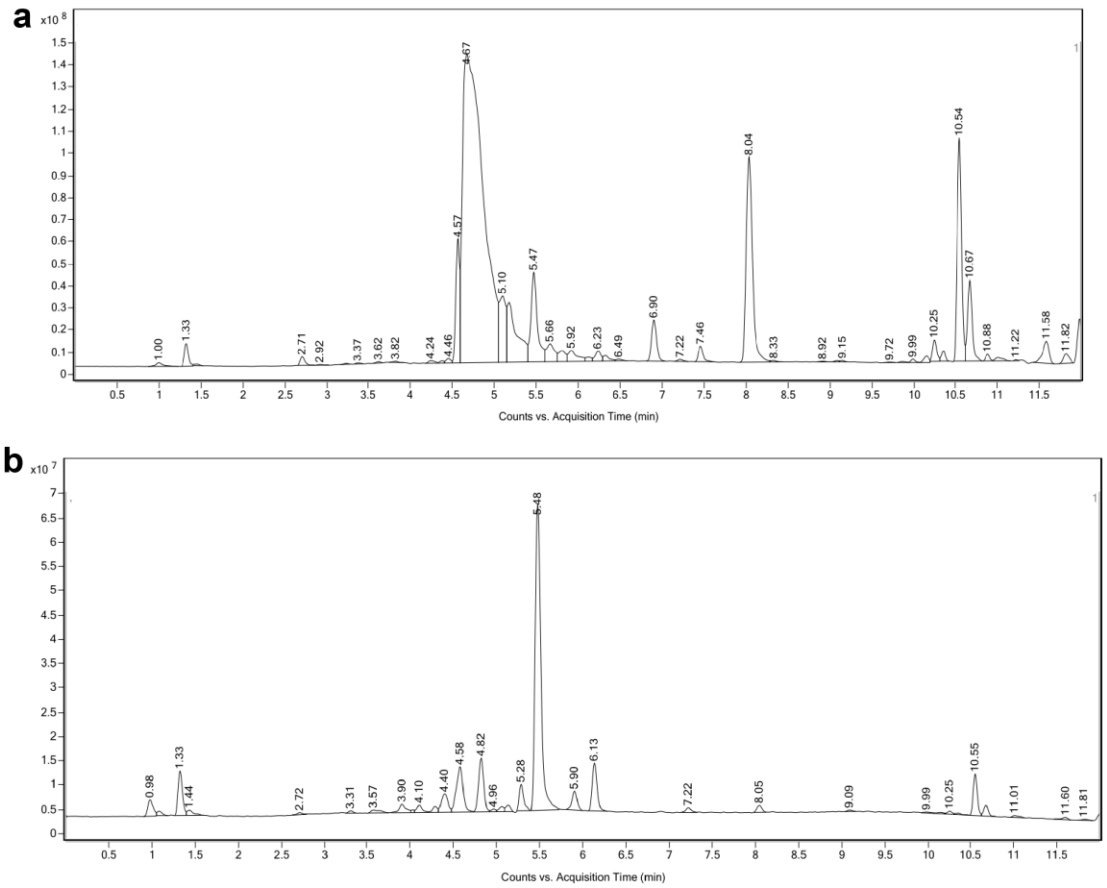

Fig.S26 LC-MS chromatograms of malachite green before (a) and after (b) degradation by DNA-Au/Pt nanozyme

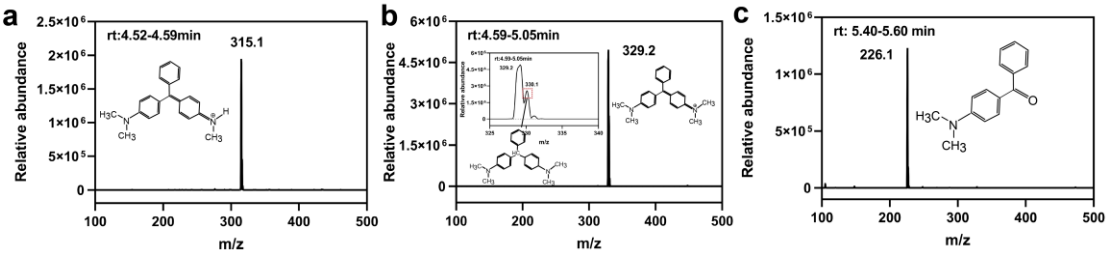

Fig.S27 The LC-MS analysis of MG. Retention time: (a)4.57 min; (b)4.76 min; (c)5.47 min

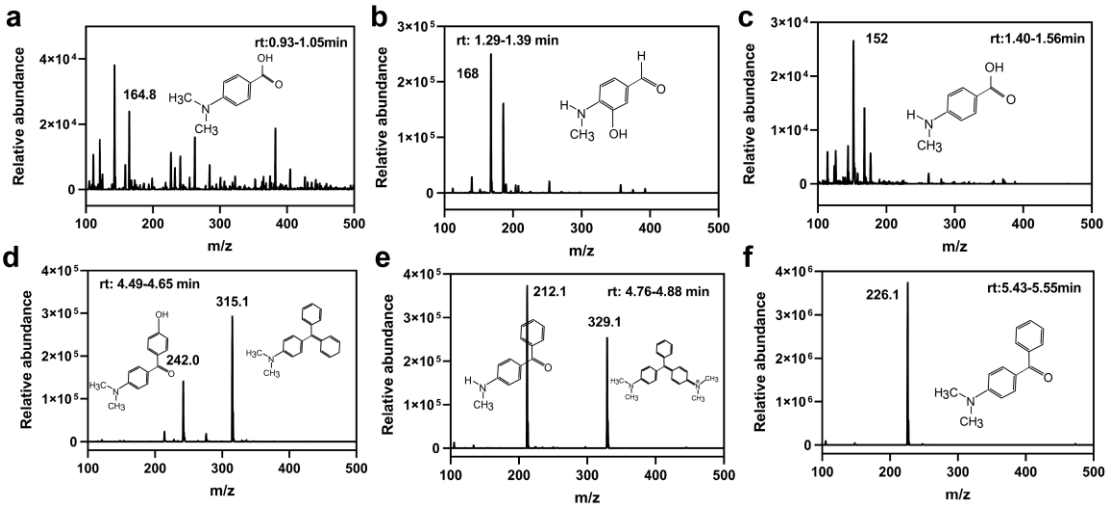

Fig. S28 The LC-MS analysis of MG after degradation by DNA-Au/Pt nanozyme. Retention time: (a)0.98 min; (b)1.33 min; (c)1.44 min; (d)4.58 min; (e)4.82 min; (f)5.48 min

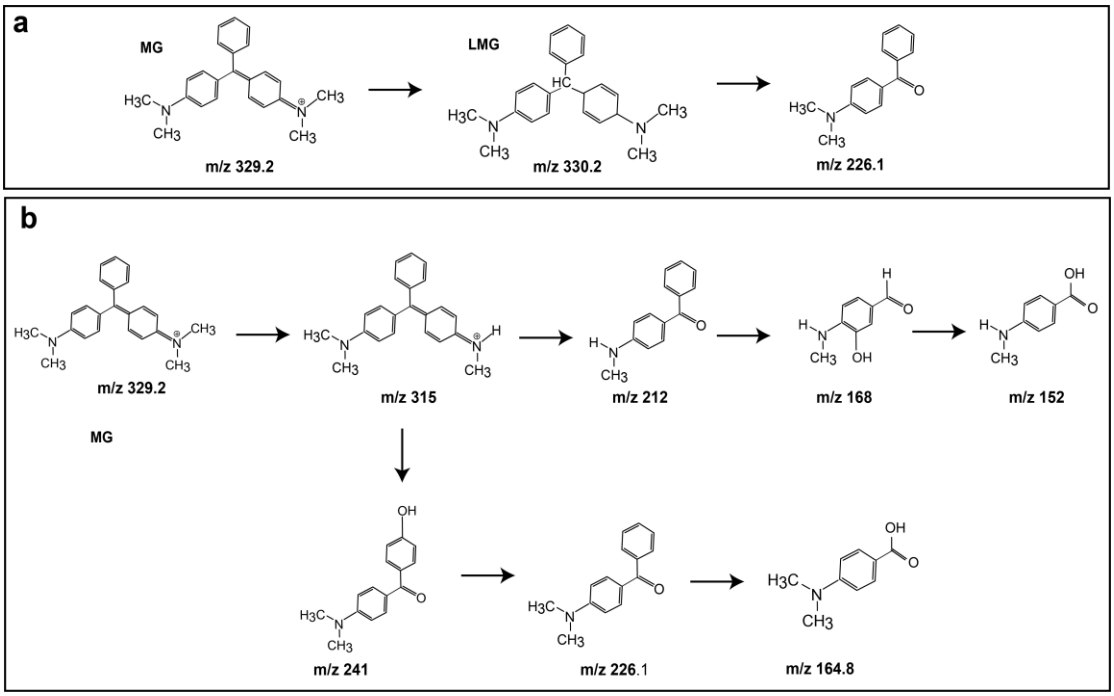

Fig. S29 Proposed pathway for MG degradation (a) natural conditions; (b) DNA-Au/Pt

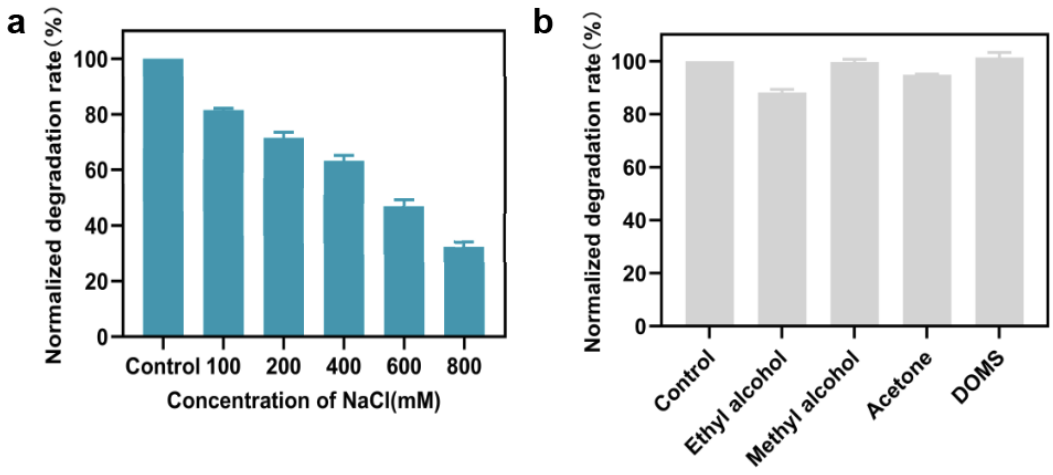

Fig. S30 The effects of ionic strength and organic solvents on the catalytic degradation of MG by DNA-Au/Pt. (a) Influence of ionic strength on MG degradation efficiency by DNA-Au/Pt nanozyme at various NaCl concentrations (Control: nanozyme+H_2O_2+MG+H_2O). (b) Effect of organic solvents (20%) on the degradation efficiency of MG by DNA-Au/Pt nanozyme (Control: nanozyme+H_2O_2+MG+H_2O)

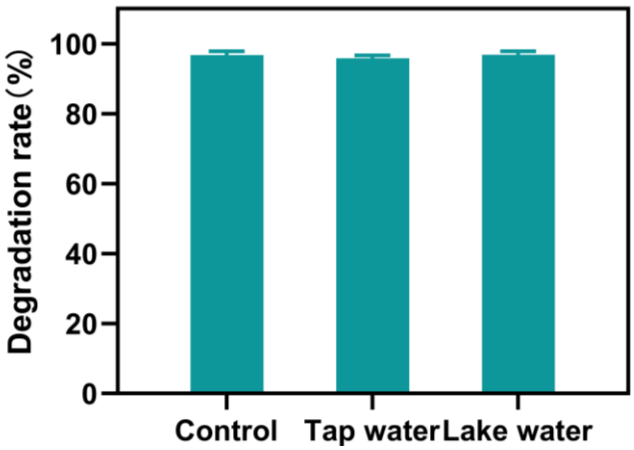

Fig. S31 The degradation ability towards MG in real wastewater (Lake water: Kunming lake)

Table S1. Nucleic acid sequences used in this work.

Name	Sequence (5'-3')
N_A	AAAAAAAAAAAA
N_T	TTTTTTTTTTTT
N_C	CCCCCCCCCCCC
N_G	GGGGGGGGGGGG
N1	CCTCCTTCCTCC
N2	ACACGAACCG
N3	CCCCCCCCCC
N4	CCCCCTAATTCCC
N5	AGGTCGCCGCCC
N6	CCCTTAATCCCC
S1	ACATACATCTATTGTATAATCCTCCTTCCTCC
S2	ACATACATCTATTGTATAATACACGAACCG
S3	ACATACATCTATTGTATAATCCCCCCCCCC
S4	ACATACATCTATTGTATAATCCCCCTAATTCC C
S5	ACATACATCTATTGTATAATAGGTCGCCGCCC
S6	ACATACATCTATTGTATAATCCCTTAATCCCC
S7	ACATACATCTATTGTATAATCCCCAAAACCC
S8	ACATACATCTATTGTATAATCCCCCTAATTCCCCC
H1-N	AAATGTAGTTTTCTACATTTCCTCCTTCCTCC
H2-N	AAATGTAGTTTTCTACATTTACACGAACCG
H3-N	AAATGTAGTTTTCTACATTTCCCCCCCCCC
H4-N	AAATGTAGTTTTCTACATTTCCCCCTAATTCC C
H1-2N	CCTCCTTCCTCCAAATGTAGTTTTCTACATTTCCTCCTTCCTCC
H2-2N	ACACGAACCG AAATGTAGTTTTCTACATTTACACGAACCG
H3-2N	CCCCCCCCCCCAAATGTAGTTTTCTACATTTCCCCCCCCCC
H4-2N	CCCCCTAATTCC CAAATGTAGTTTTCTACATTTCCCCCTAATTCC C
A5	AAAAACTACATTATACAATAGATGTATGT

A10	AAAAAAAAAACTACATTATACAATAGATGTATGT
A20	AAAAAAAAAAAAAAAAAAACTACATTATACAATAGATGTATGT
A30	AAAAAAAAAAAAAAAAAAAAAAAAAAAAACTACATTATACAATAGATGTATGT
T5	TTTTTCTACATTATACAATAGATGTATGT
T10	TTTTTTTTTTCTACATTATACAATAGATGTATGT
T20	TTTTTTTTTTTTTTTTTTTTCTACATTATACAATAGATGTATGT
T30	TTTTTTTTTTTTTTTTTTTTTTTTTTTTTTCTACATTATACAATAGATGTATGT
C5	CCCCCTACATTATACAATAGATGTATGT
C10	CCCCCCCCCCCTACATTATACAATAGATGTATGT
C20	CCCCCCCCCCCCCCCCCCCCCCCCTACATTATACAATAGATGTATGT
C30	CCCCCCCCCCCCCCCCCCCCCCCCCCCCCCCCCCCCTACATTATACAATAGATGTATGT
G_5-rich	GGGGGCTACATTATACAATAGATGTATGT
G_{10}-rich	GGGGGTGGGGGCTACATTATACAATAGATGTATGT
G_{20}-rich	GGGGGTGGGGGTGGGGGTGGGGGCTACATTATACAATAGATGTATGT
G_{30}-rich	GGGGGTGGGGGTGGGGGTGGGGGTGGGGGTGGGGGCTACATTATACAATAGATGTATGT
DNAzyme	CACTTCTTCAACATCAGTCTGATAAGCTATTTCCTTGGGGAAAGGCTAGCTACAACGAAGAAGTG
H-Bio	Biotin-ACACGAACCGACTTCAACCCACTTCT/rA//rU/TTTCCCCAAGGTTGAAGAA
HC-0-2-4	TTTCCCCGAAGAA
HC-2-2-4	TTTCCCCAAGAAGAA
HC-4-2-4	TTTCCCCAAGGGAAGAA
HC-8-2-4	TTTCCCCAAGGAAGAAGAA
HC-4-0-4	TTTCCCCAAGGAGAA
HC-4-2-4	TTTCCCCAAGGGAAGAA
HC-4-4-4	TTTCCCCAAGGTTGAAGAA
HC-4-6-4	TTTCCCCAAGGTGTTGAAGAA
HC-4-4-0	TTTCCCCAAGGTTGA
HC-4-4-2	TTTCCCCAAGGTTGAAG
HC-4-4-4	TTTCCCCAAGGTTGAAGAA
HC-4-4-7	TTTCCCCAAGGTTGAAGAAGTG
miRNA-21	UAGCUUAUCAGACUGAUGUUGA
miRNA-155	UUAAUGCUAAUCGUGAUAGGGGU

miRNA-103a	AGCAGCAUUGUACAGGGCUAUGA
miRNA-m5	UAGCAUAUCAGACUGAUGUUGA
miRNA-m11	UAGCUUAUCACACUGAUGUUGA
miRNA-m21	UAGCUUAUCAGACUGAUGUUAA

Table S2. Comparison of *K*m and *V*max between DNA-Au/Pt nanozymes and other Au or Pt-based peroxidase-mimicking nanozymes.

Nanozyme	Substance	*K*m (mM)	*V*max (10^{-8}Ms^{-1})	Ref.
Au	TMB	3.59	0.861	[1]
	H_2O_2	16.71	7.386	
Pt	TMB	0.1206	6.51	[2]
	H_2O_2	205.6	9.79	
DNA-Pt	TMB	0.056	58.2	[3]
	H_2O_2	48	56.8	
Au@Ag-hemin-reduced graphene	TMB	0.048	28.07	[4]
	H_2O_2	2.75	15.3	
Au/CeO_2	TMB	0.29	3.9	[5]
	H_2O_2	44.69	2.23	
Au-Fe_2O_3	TMB	0.0429	5.882	[6]
	H_2O_2	138.5	4.770	
Pd@Pt	TMB	0.43	5.1	[7]
	H_2O_2	14	9.0	
Pt-Ir	TMB	0.38	3.4	[8]
	H_2O_2	4.13	2.60	
Au@Pt	TMB	0.285	2.96	[9]
	H_2O_2	0.341	2.51	
Au@Pt	TMB	0.3	19.51	[10]
	H_2O_2	10.67	12.56	
Au@Pt	TMB	0.03	5.5	[11]
	H_2O_2	13.22	5.2	
Au@Pd@Pt	TMB	0.065	24.78	[12]
	H_2O_2	4.59	19.82	
DNA-Au/Pt	TMB	7.37	10.66	This work
	H_2O_2	0.26	9.66	

Table S3. Comparison of miRNA detection based on nanozyme.

Nanozyme	Synthesis time	Limit of detection	Linear range	Detection time	Ref.
Ru@TiO_2	25h	100 pM	1-20 μM	70min	[13]
DNA @CeO_2@Au	10h	6.8 pM	0-100 nM	1 h	[14]
CeO_2-TiO_2 NTs-CFPE	37h	0.6 fM	2 fM-170 pM	3 h	[15]
Pt@Au	0.5h	0.5 pM	1 pM-500 pM	1.5h	[16]
MoS_2-Au@Pt	0.4h	0.7 aM	10 pM-100 nM	5.6 h	[17]
Cu SAs@CN	80h	1.09 fM	10 fM-500 nM	2.5h	[18]
DNA-Au/Pt	1h	0.2 pM	10 pM-100 nM	2.5 h	This work

Table S4. Comparison of miRNA colorimetric detection based on DNAzyme.

Method	Limit of detection	Linear range	Detection time	Selectivity	Ref.
DNAzyme-RCA	1 pM	1 pM-100 nM	3h	other miRNAs	[19]

G-quadruplex DNAzyme decorated spherical nucleic acid	0.7 nM	1 - 100 nM	~1h	Two- base mismatch	[20]
G-quadruplex/hemin DNAzymes	90.3 fM	100 fM-20 nM	1 h	Single-base mismatch	[21]
G3/hemin DNAzyme-based RCA	2.9 pM	0 pM-500 pM	~1.5h	Single-base mismatch	[22]
CRISPR-Cas13a-Triggered DNAzyme	27 fM	50 fM - 1 nM	~1h	other miRNAs	[23]
DNA-Au/Pt	0.2 pM	10 pM-100 nM	2.5 h	Single-base mismatch	This work

Table S5. Recovery of miR-21 in human serum sample(n=3).

Samples	Input (nM)	Output (nM)	Recovery (%)	RSD[a] (±%)
1	0.01	0.0102	102%	2.95%
2	0.1	0.099	99%	6.53%
3	1	0.986	98.6%	4.66%
4	2	2.13	106.5%	4.32%

RSD[a]: relative standard deviation.

References

1. Hu LZ, Liao H, Feng LY, Wang M, Fu WS (2018) Accelerating the Peroxidase-Like Activity of Gold Nanoclusters at Neutral pH for Colorimetric Detection of Heparin and Heparinase Activity. Anal Chem 90:6247-52. https://doi.org/10.1021/acs.analchem.8b00885
2. Wu GW, He SB, Peng HP, Deng HH, Liu AL, Lin XH, Xia XH, Chen W (2014) Citrate-Capped Platinum Nanoparticle as a Smart Probe for Ultrasensitive Mercury Sensing. Anal Chem 86:10955-60. https://doi.org/10.1021/ac503544w
3. Fu Y, Zhao XY, Zhang JL, Li W (2014) DNA-Based Platinum Nanozymes for Peroxidase Mimetics. J Phys Chem C 118:18116-25. https://doi.org/10.1021/jp503242e
4. Kumar S, Bhushan P, Bhattacharya S (2017) Facile synthesis of Au@Ag-hemin decorated reduced graphene oxide sheets: a novel peroxidase mimetic for ultrasensitive colorimetric detection of hydrogen peroxide and glucose. Rsc Adv 7:37568-77. https://doi.org/10.1039/c7ra06973a
5. Bhagat S, Vallabani NVS, Shutthanandan V, Bowden M, Karakoti AS, Singh S (2018) Gold core/ceria shell-based redox active nanozyme mimicking the biological multienzyme complex phenomenon. J Colloid Interface Sci 513:831-42. https://doi.org/10.1016/j.jcis.2017.11.064
6. Masud MK, Yadav S, Isam MN, Nguyen NT, Salomon C, Kline R, Alamri HR, Alothman ZA, Yamauchi Y, Hossain MSA, Shiddiky MJA (2017) Gold-Loaded Nanoporous Ferric Oxide Nanocubes with Peroxidase-Mimicking Activity for Electrocatalytic and Colorimetric Detection of Autoantibody. Anal Chem 89:11005-13. https://doi.org/10.1021/acs.analchem.7b02880
7. Wu RF, Chong Y, Fang G, Jiang XM, Pan Y, Chen CY, Yin JJ, Ge CC (2018) Synthesis of Pt Hollow Nanodendrites with Enhanced Peroxidase-Like Activity against Bacterial Infections: Implication for Wound Healing. Adv Funct Mater 28:1801484. https://doi.org/10.1002/adfm.201801484
8. Yang HY, He QY, Pan JK, Shen D, Xiao HX, Cui XP, Zhao SQ (2021) A Pt-Ir nanocube amplified lateral flow immunoassay for dehydroepiandrosterone. Analyst 146:2726-33. https://doi.org/10.1039/d0an02293d
9. Qiao WL, He BS, Yang J, Ren WJ, Zhao RY, Zhang YR, Bai CQ, Suo ZG, Xu YW, Wei M, Jin HL (2024) Pt@AuNF nanozyme and horseradish peroxidase-based lateral flow immunoassay dual enzymes signal amplification strategy for sensitive detection of zearalenone. Int J Biol Macromol 254:127746. https://doi.org/10.1016/j.ijbiomac.2023.127746
10. Long L, Liu JB, Lu KS, Zhang T, Xie YQ, Ji YL, Wu XC (2019) Highly sensitive and robust peroxidase-like activity of Au-Pt core/shell nanorod-antigen conjugates for measles virus diagnosis (vol 16, 46, 2018). J Nanobiotechnology 17:4. https://doi.org/10.1186/s12951-018-0435-1

11. Lu C, Tang LH, Gao F, Li YZ, Liu JW, Zheng JK (2021) DNA-encoded bimetallic Au-Pt dumbbell nanozyme for high-performance detection and eradication of Escherichia coli O157:H7. Biosens Bioelectron 187:113327. https://doi.org/10.1016/j.bios.2021.113327
12. Sun Y, Xie ZH, Pei FB, Hu W, Feng SS, Hao QL, Liu B, Mu XH, Lei W, Tong ZY (2022) Trimetallic Au@Pd@Pt nanozyme-enhanced lateral flow immunoassay for the detection of SARS-CoV-2 nucleocapsid protein. Anal Methods 14:5091-9. https://doi.org/10.1039/d2ay01530g
13. Zhang LM, He X, Bai H, Yu XZ, Wu PL, Cai ZW, Ren YC, Luo YS, Zhuang WH, Hu J, Ying BW, Luo FM, Yao YC, Sun XP, Hu WC (2024) On-Site Visualization Assay for Tumor-Associated miRNAs: Using Ru@TiO_2 as a Peroxidase-like Nanozyme. Anal Chem 96:16499-504. https://doi.org/10.1021/acs.analchem.4c03922
14. Yu JY, Liu QY, Qi LJ, Fang Q, Shang XD, Zhang XJ, Du Y (2024) Fluorophore and nanozyme-functionalized DNA walking: A dual-mode DNA logic biocomputing platform for microRNA sensing in clinical samples. Biosens Bioelectron 252:116137. https://doi.org/10.1016/j.bios.2024.116137
15. Li L, Zhang Y, Yan Z, Chen MQ, Zhang LN, Zhao PN, Yu JH (2020) Ultrasensitive Photoelectrochemical Detection of MicroRNA on Paper by Combining a Cascade Nanozyme-Engineered Biocatalytic Precipitation Reaction and Target-Triggerable DNA Motor. Acs Sensors 5:1482-90. https://doi.org/10.1021/acssensors.0c00632
16. Luo B, Zhou J, Zhan XH, Ying BW, Lan F, Wu Y (2024) Visual and colorimetric detection of microRNA in clinical samples based on strand displacement amplification and nanozyme-mediated CRISPR-Cas12a system. Talanta 277:126310. https://doi.org/10.1016/j.talanta.2024.126310
17. Ma JF, Yao QY, Lv S, Yi JS, Zhu D, Zhu CF, Wang LH, Su S (2024) Integrated triple signal amplification strategy for ultrasensitive electrochemical detection of gastric cancer-related microRNA utilizing MoS_2-based nanozyme, hybridization chain reaction, and horseradish peroxidase. J Nanobiotechnology 22:596. https://doi.org/10.1186/s12951-024-02848-z
18. Liu RF, Li CX, Zhu LF, Wang SJ, Liu DD, Xie L, Ge SG, Yu JH (2024) Cu Single-Atom Nanozyme-Mediated Electrochemiluminescence Biosensor for Highly Sensitive Detection of MicroRNA-622. Anal Chem 96:12838-45. https://doi.org/10.1021/acs.analchem.4c02514
19. Zhang H, Tang Y, Zhou YS, Wang YG, Si HB, Li L, Tang B (2024) DNAzyme-RCA-based colorimetric and lateral flow dipstick assays for the point-of-care testing of exosomal m5C-miRNA-21. Chem Sci 15:9345-52. https://doi.org/10.1039/d4sc02648a
20. Shahsavar K, Shokri E, Hosseini M (2022) Sensitive colorimetric detection of miRNA-155 via G-quadruplex DNAzyme decorated spherical nucleic acid. Microchim Acta 189:357. https://doi.org/10.1007/s00604-022-05455-7
21. Yang XJ, Yuan LQ, Xu Y, He BF (2023) Target-catalyzed self-assembled spherical G-quadruplex/hemin DNAzymes for highly sensitive colorimetric detection of microRNA in

serum. Anal Chim Acta 1247:340879. https://doi.org/10.1016/j.aca.2023.340879

22. Li RY, Liu Q, Jin Y, Li BX (2020) Sensitive colorimetric determination of microRNA let-7a through rolling circle amplification and a peroxidase-mimicking system composed of trimeric G-triplex and hemin DNAzyme. Microchim Acta 187:139. https://doi.org/10.1007/s00604-019-4093-2
23. Yan N, Hu ZW, Zhang LL (2024) CRISPR-Cas13a-Triggered DNAzyme Signal Amplification-Based Colorimetric miRNA Detection Method and Its Application in Evaluating the Anxiety. Appl Biochem Biotechnol. https://doi.org/10.1007/s12010-024-04951-1